




Fibroblast mTOR/PPAR γ /HGF axis protects against tubular cell death and acute kidney injury

Yuan Gui¹ · Qingmiao Lu¹ · Mengru Gu¹ · Mingjie Wang¹ · Yan Liang¹ · Xingwen Zhu¹ · Xian Xue¹ · Xiaoli Sun¹ · Weichun He¹ · Junwei Yang¹ · Allan Zijian Zhao² · Bo Xiao³ · Chunsun Dai¹ 

Received: 14 November 2018 / Revised: 8 April 2019 / Accepted: 11 April 2019 / Published online: 25 April 2019
© ADMC Associazione Differenziamento e Morte Cellulare 2019

Abstract

Kidney fibroblasts play a crucial role in dictating tubular cell fate and the outcome of acute kidney injury (AKI). The underlying mechanisms remain to be determined. Here, we found that mTOR signaling was activated in fibroblasts from mouse kidneys with ischemia/reperfusion injury (IRI). Ablation of fibroblast Rheb or Rictor promoted, while ablation of fibroblast Tsc1 protected against tubular cell death and IRI in mice. In tubular cells cultured with conditioned media (CM) from Rheb^{-/-} or Rictor^{-/-} fibroblasts, less hepatocyte growth factor (HGF) receptor c-met signaling activation or staurosporine-induced cell apoptosis was observed. While CM from Tsc1^{-/-} fibroblasts promoted tubular cell c-met signaling activation and inhibited staurosporine-induced cell apoptosis. In kidney fibroblasts, blocking mTOR signaling downregulated the expression of peroxisome proliferator-activated receptor gamma (PPAR γ) and HGF. Downregulating fibroblast HGF expression or blocking tubular cell c-met signaling facilitated tubular cell apoptosis. Notably, renal PPAR γ and HGF expression was less in mice with fibroblast Rheb or Rictor ablation, but more in mice with fibroblast Tsc1 ablation than their littermate controls, respectively. Together, these data suggest that mTOR signaling activation in kidney fibroblasts protects against tubular cell death and dictates the outcome of AKI through stimulating PPAR γ and HGF expression.

Introduction

Acute kidney injury (AKI), caused by ischemia/reperfusion, sepsis or nephrotoxins, is a worldwide health problem [1, 2]. Regardless of the causes, tubular cell death or detachment from the tubular base membrane will lead to the

back leak of glomerular filtrate from the tubular lumen to the interstitium and kidney dysfunction. After injury, the viable tubular cells may undergo dedifferentiation, migration, and proliferation to replace dead tubular cells [3–7]. Elucidating the mechanisms of tubular cell death and exploring new strategy for promoting tubular cell survival will benefit patients suffering from AKI [8].

Except for playing an essential role in kidney fibrogenesis, fibroblasts resided between the capillaries and tubule may regulate tubular cell survival, repair and regeneration [9, 10]. Kramann et al. reported that loss of fibroblasts/pericytes induces proximal tubular injury [11]. Schiessl et al. found that renal interstitial PDGFR β positive cells may promote proximal tubular cell regeneration [12]. Recently, Zhou et al. demonstrated that fibroblast β -catenin signaling activation facilitates tubular cell death through suppressing fibroblast Hepatocyte growth factor (HGF) production [13]. Therefore, manipulating intrinsic signaling pathways of kidney fibroblasts may provide a new strategy for preventing tubular cell death and AKI.

The mammalian Target of Rapamycin (mTOR) participates into forming two distinct complexes, named mTOR

Edited by D. Vaux

Supplementary information The online version of this article (<https://doi.org/10.1038/s41418-019-0336-3>) contains supplementary material, which is available to authorized users.

✉ Chunsun Dai
daichunsun@njmu.edu.cn

- ¹ Center for Kidney Disease, 2nd Affiliated Hospital, Nanjing Medical University, 262 North Zhongshan Road, Nanjing, Jiangsu, China
- ² Institute of Biomedical and Pharmaceutical Sciences, Guangdong University of Technology, 510515 Guangzhou, China
- ³ Neuroscience and Metabolism Research, the State Key Laboratory of Biotherapy, West China Hospital, Sichuan University, 610041 Chengdu, China

complex 1 (mTORC1) and mTOR complex 2 (mTORC2) [14–16]. Rheb, a small GTPase, is a crucial activator for mTORC1 signaling [17, 18]. Tsc1, a stabilizer for Tsc2 which functions as a GTPase-activating protein for Rheb, inhibits Rheb and mTORC1 signaling activation [19, 20]. Rictor is an adapter protein and kinase regulator for mTORC2 and deficiency of which results in reduced mTORC2 activity [21]. The published studies reported that both mTORC1 and mTORC2 activation in tubular cells protect against tubular cell death and AKI [22, 23]. In addition, activation of mTORC1 or mTORC2 in fibroblasts promotes fibroblast activation and kidney fibrosis in mice with unilateral ureter obstruction (UO) nephropathy [24, 25]. However, the role and mechanisms for fibroblast mTORC1 and mTORC2 activation in regulating tubular cell survival and AKI are not clear.

In this study, we demonstrated that fibroblast mTORC1 and mTORC2 signaling are crucial for protecting against tubular cell death and ischemia/reperfusion injury (IRI)-induced AKI through stimulating PPAR γ and HGF expression. Our studies illustrate a novel role and mechanism for fibroblast mTOR signaling in regulating tubular cell survival and AKI.

Materials and methods

Mouse models

Rheb^{fl/fl} mice were provided by Dr. Xiao from Sichuan University [26]. Tsc1^{fl/fl} mice were ordered from Jackson Laboratory (cat: 005680, Jackson Labs, Bar Harbor, ME). Rictor^{fl/fl} mice were provided by Dr. Magnuson from University of Vanderbilt. Mice with genotypes Gli1-Cre^{+/-}, Rheb^{fl/fl}; Gli1-Cre^{+/-}, Tsc1^{fl/fl}; and Gli1-Cre^{+/-}, Rictor^{fl/fl} were generated by cross breeding Gli1-CreERT2 transgenic mice (cat: 007913, Jackson Labs) [27] with Rheb^{fl/fl}, Tsc1^{fl/fl}, and Rictor^{fl/fl} mice, respectively (all were on C57BL/6J background). The same gender litters with genotypes Gli1-Cre^{-/-}, Rheb^{fl/fl}; Gli1-Cre^{-/-}, Tsc1^{fl/fl}; and Gli1-Cre^{-/-}, Rictor^{fl/fl} were considered as littermate controls, respectively. Male mice at 10 weeks of age were intraperitoneally injected with tamoxifen (cat: T5648, Sigma-Aldrich, St. Louis, MO) at 25 mg/kg for 5 consecutive days to induce target gene ablation. At day 2 after the last injection, the left renal pedicles were clamped for 25 min and reperfused within 1 min. The right kidneys were removed immediately after reperfusion. The mouse body temperature was maintained at 36.5–37.5 °C during I/R surgery [28].

Male CD-1 mice (18–20 g) acquired from the Specific Pathogen-Free Laboratory Animal Center of Nanjing

Medical University were performed with left renal IRI and right renal nephrectomy as described above.

All animals were maintained in the Specific Pathogen-Free Animal Center of Nanjing Medical University according to the guidelines of the Institutional Animal Care and Use Committee at Nanjing Medical University.

Cell culture

Normal rat kidney fibroblasts (NRK-49F) and Normal rat kidney tubular epithelial cells (NRK-52E) were ordered from ATCC (Manassas, VA). Fibroblasts isolated from kidney cortex of Rheb^{fl/fl}, Tsc1^{fl/fl}, or Rictor^{fl/fl} mice were cultured with EMEM containing 10% FBS and infected with adenovirus carrying Cre recombinase gene to generate fibroblast Rheb, Tsc1, or Rictor ablation, respectively. Tubular cells isolated from kidney cortex of wide-type mice were cultured with DMEM/F12 supplemented with 10% FBS (Invitrogen, Grand Island, NY). Fibroblasts were treated with PP242 (cat: P0037, Sigma-Aldrich, St. Louis, MO), Pioglitazone (Absin, Shanghai, China), PF-04217903 (T2676, Targetmol, Shanghai, China), or staurosporine (S4400, Sigma-Aldrich, St. Louis, MO) as indicated. NRK-49F cells were transfected with HGF siRNAs (Integrated Biotech Solutions, Shanghai, China) using Lipofectamine 2000 reagent (Invitrogen, Grand Island, NY) according to the manufacturer's instruction.

Histology and immunohistochemical staining

Kidney tissues were fixed with 10% neutral formalin solution. For immunohistochemical staining, kidney sections at 3- μ m thickness were incubated with antibody against PPAR γ (cat: SAB4502262, Sigma-Aldrich, St. Louis, MO).

Immunofluorescent staining

Kidney cryosections at 3- μ m thickness were fixed with 4% paraformaldehyde for 15 min, followed by permeabilization with 0.2% Triton X-100 in 1 \times PBS for 5 min at RT. After blocking with 2% normal donkey serum for 60 min, the slides were immunostained with antibodies against Gli1 (cat: 388516, RD Systems), Fsp1 (cat: NB100-55404, Novus), PDGFR β (cat:14-1402, eBioscience), p-Akt (Ser473) (cat: 3868, Cell Signaling Technology), p-S6 (cat: 4858, Cell Signaling Technology), Rheb (cat: ab25873, abcam), Tsc1 (cat: 4906, Cell Signaling Technology), Rictor (cat: A300-459A, Bethyl Laboratories), cleaved caspase 3 (cat: 9664, Cell Signaling Technology), Ly6b (cat: MCA771G, AbD Serotec, Raleigh, NC), and CD3 (cat: 555273, BD Pharmingen), respectively. Primary cultured tubular cells and NRK-52E cells seeded on

coverslips were fixed with methanol/acetone (1:1) for 10 min at -20°C . After three extensive washings with $1\times$ PBS, the coverslips were incubated with 2% normal donkey serum for 40 min at RT, then incubated with anti-cleaved caspase 3 overnight, followed by incubation with fluorescein isothiocyanate or tetramethylrhodamine-conjugated secondary antibody. Cells were stained with 4', 6-diamidino-2-phenylindole and viewed with a Nikon Eclipse 80i Epi-fluorescence microscope equipped with a digital camera.

TUNEL staining

Terminal deoxynucleotidyl transferase-mediated dUTP nick-end labeling staining was employed to determine apoptotic cells by using the apoptosis detection system (Promega, Madison, WI).

Western blot analysis

Primary cultured tubular cells and NRK-52E cells were lysed in $1\times$ SDS buffer. Kidney tissues were lysed with RIPA solution containing 1% NP40, 0.1% SDS, 100 $\mu\text{g}/\text{ml}$ PMSF, 1% protease inhibitor cocktail, and 1% phosphatase I and II inhibitor cocktails (Sigma, St Louis, MO) on ice for 30 min. The supernatants were collected after centrifugation at 13,000 g at 4°C for 30 min. Protein concentration was determined by the bicinchoninic acid protein assay (BCA Kit; Pierce Thermo-Scientific, Rockford, IL) according to the manufacturer's instruction. Equal amount of protein for each sample was loaded into sodium dodecyl sulfate-polyacrylamide gel electrophoresis and transferred onto polyvinylidene difluoride membranes. The membranes were probed with antibodies against: p-Akt (Ser473) (cat: 3868, Cell Signaling Technology), p-S6 (cat: 4858, Cell Signaling Technology), cleaved caspase 3 (cat: 9664, Cell Signaling Technology), PPAR γ (cat: SAB4502262, Sigma-Aldrich, St. Louis, MO), p-c-met (cat: 3126, Cell Signaling Technology), p-ERK1/2 (cat: 4370, Cell Signaling Technology), α -tubulin (cat: T9026, Sigma, St. Louis, MO), and GAPDH (cat: FL-335, Santa Cruz Biotechnology, Dallas, TX), respectively. Quantification was performed by measuring the signal intensity with the aid of National Institutes of Health Image J software package.

Conditioned media (CM) from cultural fibroblasts

Fibroblasts were treated for 48 h as indicated, then cultured with serum-free media for 24 h. Cultural media was harvested and centrifuged (3000 rpm for 10 min at 4°C). The supernatant was aliquot and stored at -80°C for the subsequent experiments.

Real-time qRT-PCR

Total RNA was extracted with Trizol reagent (Invitrogen) according to the manufacturer's instruction. cDNA was synthesized with 1 μg of total RNA, ReverTra Ace (Vazyme, Nanjing, China), and oligo (dT) 12–18 primers. Real-time qRT-PCR assay was used to quantitate the mRNA abundance with 7300 real-time PCR system (Applied Biosystems, Foster City, CA). The relative amount of mRNA to internal control was calculated using the equation $2^{-\Delta\text{CT}}$, in which $\Delta\text{CT} = \text{CT}_{\text{gene}} - \text{CT}_{\text{control}}$.

Statistics

All data examined are presented as mean \pm s.e.m. Statistical analyses were performed using the Graphpad Prism 6 (GraphPad Software, San Diego, CA). Comparison between groups was made using one-way analysis of variance, followed by the Student–Newman–Keuls test. $P < 0.05$ was considered as statistically significant.

Results

Both mTORC1 and mTORC2 signaling are activated in kidney fibroblasts after IRI

A mouse model with ischemia/reperfusion-induced AKI was employed in this study (Fig. 1a). Western blot assay showed that the abundance of p-Akt (Ser473) and p-S6 was largely increased at 6 and 24 h after IRI, indicating the activation of both mTORC1 and mTORC2 signaling in the kidney tissues (Fig. 1b, c). To examine whether mTOR signaling was activated in kidney fibroblasts, we costained the kidney tissues with antibodies against Gli1 and p-Akt (Ser473), Fsp1 and p-Akt (Ser473), Gli1 and p-S6, or Fsp1 and p-S6, respectively. The results showed that p-S6 and p-Akt (Ser473) were detected in Gli1 as well as Fsp1-positive cells within the IRI kidneys (Fig. 1d, e). Therefore, the results suggest that both mTORC1 and mTORC2 signaling are activated in kidney fibroblasts after IRI.

Blockade of mTORC1 signaling with Rheb ablation in fibroblasts aggravates kidney IRI in mice

To explore the role for fibroblast mTORC1 activation in IRI-induced AKI, we generated a mouse model with inducible ablation of Rheb in fibroblasts. After several times of cross breeding of Rheb floxed mice and Gli1-CreERT2 mice, we obtained mice with genotype Gli1-Cre $^{+/-}$, Rheb $^{fl/fl}$ (Supplemental Fig. 1a, lane 1). Mice were injected intraperitoneally with tamoxifen to induce Rheb ablation in fibroblasts. The same gender litters with genotype Gli1-Cre $^{-/-}$, Rheb $^{fl/fl}$ were

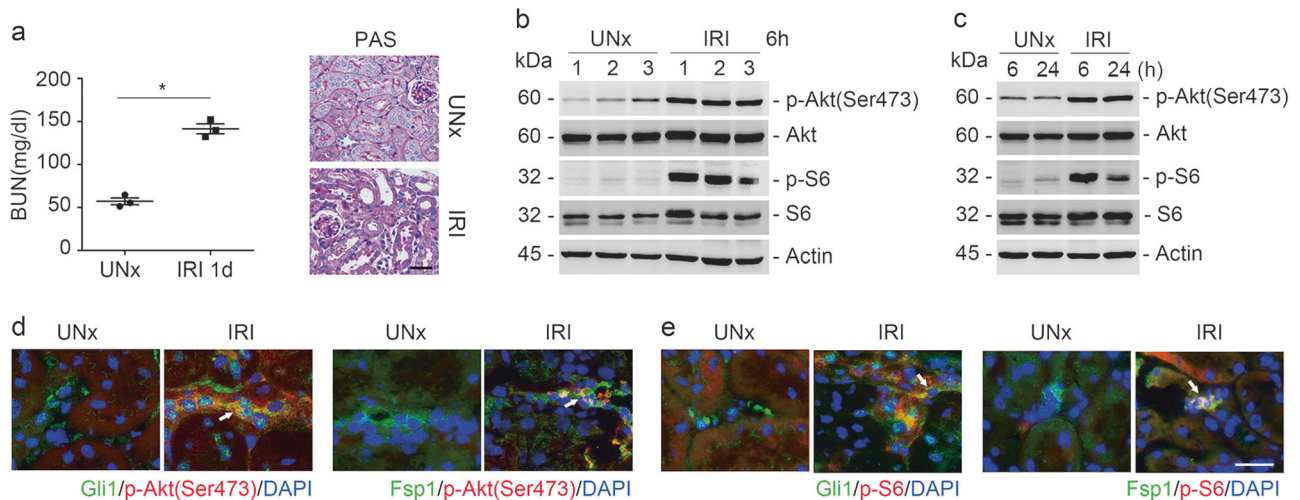


Fig. 1 Both mTORC1 and mTORC2 signaling are activated in kidney fibroblasts after IRI. **a** The graph showing the blood urea nitrogen (BUN) level in CD-1 mice at day 1 after UNx or IRI. * $P < 0.05$, $n = 3$ (left). Kidney histology as shown by periodic acid-Schiff (PAS) staining. Scale bar = 20 μ m (right). **b**, **c** Western blot analyses showing the induction of p-Akt (Ser473), and p-S6 in the kidneys after

ischemia-reperfusion injury (IRI). The numbers indicate each individual animal within the given group (**b**). The samples were pooled from three animals within each group (**c**). **d** Representative images showing the induction for p-Akt (Ser473) and p-S6 in Gli1- or Fsp1-positive fibroblasts from the IRI kidneys. White arrows indicate the co-staining positive cells. Scale bar = 20 μ m

injected with tamoxifen and treated as littermate controls (Fig. 2a). Body weight, kidney weight, kidney weight/body weight ratio, and the level of blood urea nitrogen (BUN) were similar between the knockouts and littermate controls (Supplemental Fig. 1b). Mice were operated with left renal IRI and right renal nephrectomy and killed at 1 day after surgery (Fig. 2a). Immunostaining results showed that Rheb abundance was largely reduced in fibroblasts from the knockouts compared to those from littermate controls (Fig. 2b). The knockouts developed more severe kidney dysfunction and morphological injury after IRI compared to their littermate controls (Fig. 2c, d, f).

We then assessed the inflammatory response in the IRI kidneys. The kidney tissues were immunostained with antibodies against Ly6b and CD3 to identify neutrophil and T lymphocyte, respectively. At 1 day after IRI, much more neutrophil and T lymphocyte infiltration was observed in the knockout kidneys compared to their littermate controls (Fig. 2d, g, h). Real-time qRT-PCR assay showed that the mRNA abundance for *Rantes*, *Mcp-1*, and *Tnf- α* was largely upregulated in the knockout kidneys compared to their littermate controls (Fig. 2i).

To determine tubular cell apoptosis, we costained kidney tissues with antibodies against cleaved caspase 3 and laminin. At 1 day after IRI, the number of cleaved caspase 3 positive tubular cells was significantly increased in the knockout kidneys compared to their littermate controls (Fig. 2e, j). TUNEL staining revealed the similar results (Fig. 2e, k). Together, it is concluded that ablation of Rheb in fibroblasts promotes tubular cell death and AKI in mice.

Activation of mTORC1 signaling with Tsc1 ablation in fibroblasts protects against kidney IRI in mice

The above data demonstrated that ablation of Rheb in fibroblasts promotes tubular cell death and AKI, we then want to know whether activating fibroblast mTORC1 signaling can protect against tubular cell death and AKI. In light of the role of Tsc1/2 in inhibiting Rheb activity and mTORC1 signaling, we generated a mouse model with genotype Gli1-Cre^{+/-}, Tsc1^{fl/fl} (Supplemental Fig. 1c, lane 3). The mice were injected with tamoxifen to induce Tsc1 ablation in fibroblasts as described above (Fig. 3a). No difference for body weight, kidney weight, kidney weight/body weight ratio or BUN level was observed between the knockouts and their littermate controls (Supplemental Fig. 1d). Costaining of antibodies against Gli1 and Tsc1 demonstrated the ablation of Tsc1 in fibroblasts from the knockouts (Fig. 3b). At 1 day after IRI, less BUN level or morphological injury was observed in the knockouts compared to those in their littermate controls (Fig. 3c, d, f). Neutrophil and T lymphocyte accumulation, mRNA abundance for *Rantes*, *Mcp-1*, and *Tnf- α* in the knockout kidneys were largely decreased compared to their littermate controls after IRI (Fig. 3d, g-i).

In Gli1⁺-Tsc1^{-/-} kidneys, the number of cleaved caspase 3 or TUNEL staining positive cells was remarkably reduced compared to those in their littermate controls after IRI (Fig. 3e, j, k). Together, these results reveal that activation of Rheb/mTORC1 in fibroblasts protects against tubular cell death and AKI in mice.

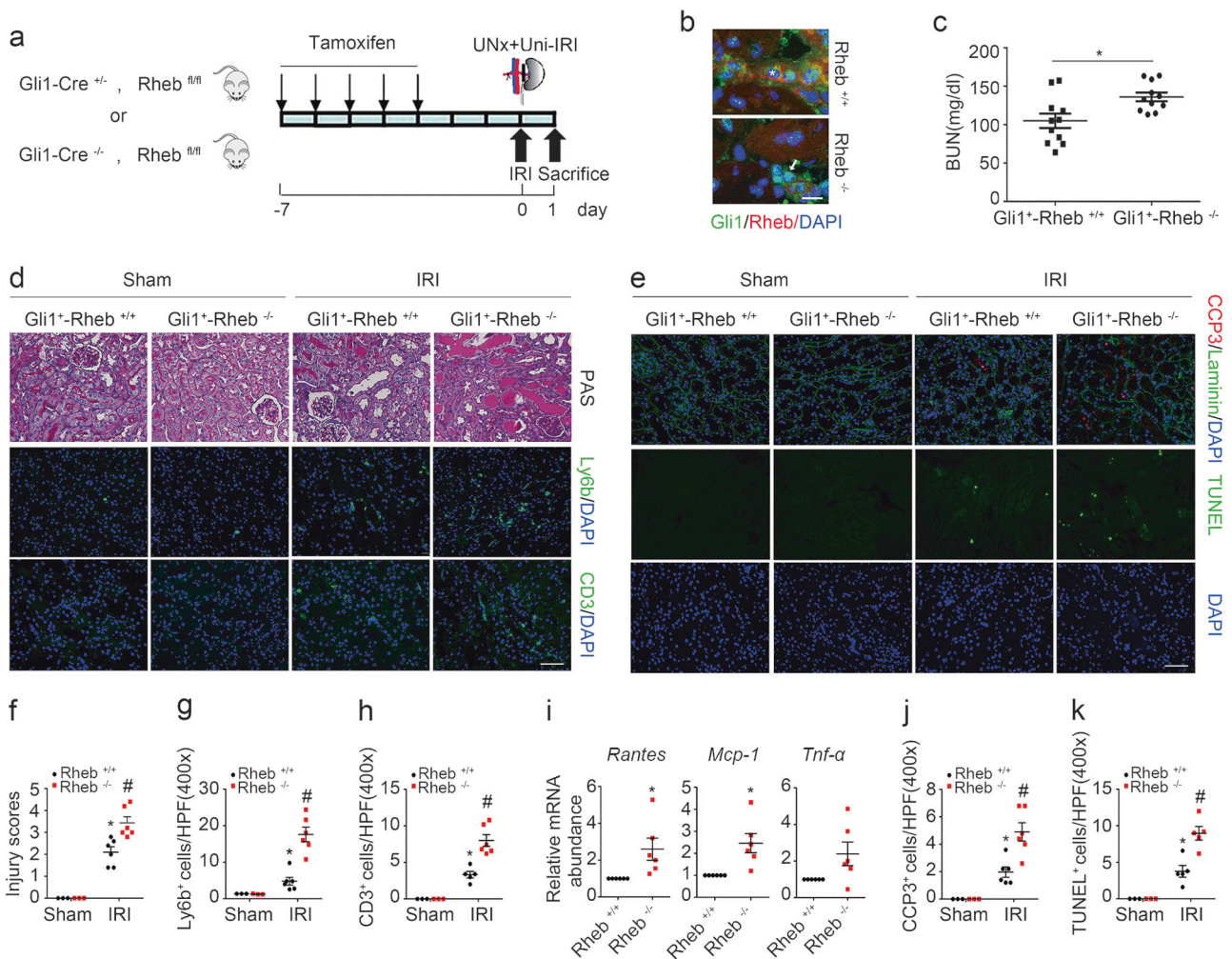


Fig. 2 Ablation of fibroblast Rheb aggravates kidney ischemia/reperfusion injury in mice. **a** The strategy for inducing fibroblast Rheb gene ablation in Gli1-Cre^{+/-}, Rheb^{fl/fl} mice and renal IRI surgery. **b** Representative micrographs showing the ablation of Rheb in Gli1⁺-Rheb^{-/-} kidneys at day 1 after IRI. The kidney tissues were immune stained with Abs against Gli1 and Rheb. The asterisk indicates both Gli1- and Rheb-positive cells in Rheb^{+/+} kidneys. The white arrow indicates Gli1-positive but Rheb-negative cells in the knockout kidneys. Scale bar = 10 μ m. **c** The graph showing the blood urea nitrogen (BUN) level in Gli1⁺-Rheb^{+/+} and Gli1⁺-Rheb^{-/-} mice at 1 day after IRI. * P < 0.05, n = 11. **d** Kidney histology as shown by PAS staining. Representative immunofluorescent staining images for Ly6b and CD3 among groups as indicated. Scale bar = 50 μ m. **e** Representative immunofluorescent staining images for cleaved caspase 3 and TUNEL staining for apoptotic cells among

groups as indicated. Scale bar = 50 μ m. **f** The graph showing the injury scores among groups. * P < 0.05 versus Rheb^{+/+} mice, n = 3–6; # P < 0.05 versus Rheb^{+/+} mice after IRI, n = 6. Each dot represents the average of five HPFs from each mouse. **g, h** Quantitative determination of Ly6b⁺ and CD3⁺ cells among groups as indicated. * P < 0.05 versus Rheb^{+/+} mice, n = 3–6; # P < 0.05 versus Rheb^{+/+} mice after IRI, n = 6. Each dot represents the average of five HPFs from each mouse. **i** Real-time qRT-PCR analysis showing the mRNA abundance for *Rantes*, *Mcp-1*, and *Tnf- α* in kidneys at day 1 after IRI. * P < 0.05 versus Rheb^{+/+} mice after IRI, n = 6. **j, k** Quantitative determination of cleaved caspase 3⁺ cells and TUNEL⁺ cells in kidneys among groups. * P < 0.05 versus Rheb^{+/+} mice, n = 3–6; # P < 0.05 versus Rheb^{+/+} mice after IRI, n = 5–6. Each dot represents the average of five HPFs from each mouse

Blockade of mTORC2 signaling with Rictor ablation in fibroblasts aggravates kidney IRI in mice

The above data demonstrated that mTORC1 signaling activation in fibroblasts plays a pivotal role in protecting against tubular cell death and AKI in mice. To explore the role for fibroblast mTORC2 signaling activation in regulating tubular cell death and AKI, we generated a mouse

model with genotype Gli1-Cre^{+/-}, Rictor^{fl/fl} (Supplemental Fig. 1e, lane 3) and the mice were injected with tamoxifen to induce fibroblast Rictor ablation (Fig. 4a). The same gender litters with genotype Gli1-Cre^{-/-}, Rictor^{fl/fl} were used as littermate controls (Supplemental Fig. 1e, lane 4). No significant difference was found for body weight, kidney weight, kidney weight/body weight ratio or BUN level between the knockouts and their littermate controls

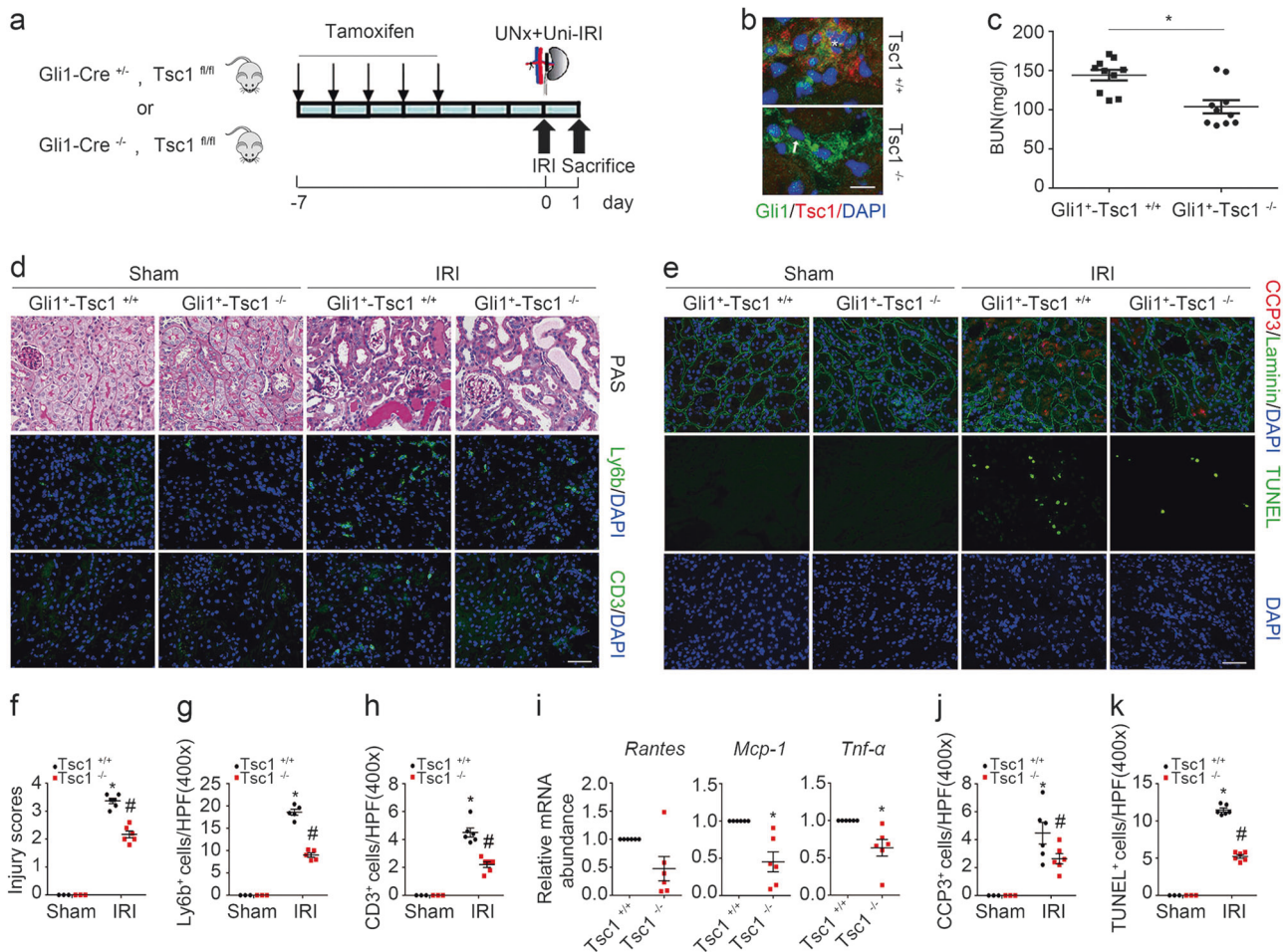


Fig. 3 Ablation of fibroblast Tsc1 protects against kidney ischemia/reperfusion injury in mice. **a** The strategy for inducing fibroblast Tsc1 gene deletion in Gli1-Cre^{+/+}, Tsc1^{fl/fl} mice and renal IRI surgery. **b** Representative immunostaining images for Gli1 and Tsc1 in the kidneys at day 1 after IRI. The kidney tissue was stained with Abs against Gli1 and Tsc1. The asterisk indicates both Gli1- and Tsc1-positive cells in Tsc1^{+/+} kidneys. The arrow indicates Gli1-positive but Tsc1-negative cells in the knockout kidneys. Scale bar = 10 μ m. **c** The graph showing the BUN level within groups at 1 day after IRI. **P* < 0.05, *n* = 10. **d** PAS staining showing that the kidney injury was attenuated in the KO mice compared to their littermate controls at day 1 after IRI. Immunofluorescent staining revealing a decreased infiltration of Ly6b⁺ neutrophils and CD3⁺ T lymphocytes in the kidneys at day 1 after IRI. Scale bar = 50 μ m. **e** Representative micrographs showing the apoptotic cells detected by immunostaining for cleaved caspase 3 and

TUNEL staining among groups. Scale bar = 50 μ m. **f** The graph showing the injury scores among groups. **P* < 0.05 versus Tsc1^{+/+} mice, *n* = 3–6; #*P* < 0.05 versus Tsc1^{+/+} mice after IRI, *n* = 6. Each dot represents the average of five HPFs from each mouse. **g, h** Quantitative determination of Ly6b⁺ and CD3⁺ cells among groups as indicated. **P* < 0.05 versus Tsc1^{+/+} mice, *n* = 3–6; #*P* < 0.05 versus Tsc1^{+/+} mice after IRI, *n* = 5–6. Each dot represents the average of five HPFs from each mouse. **i** Real-time qRT-PCR analysis showing the mRNA abundance for *Rantes*, *Mcp-1*, and *Tnf- α* in Tsc1^{+/+} and knockout kidneys at day 1 after IRI. **P* < 0.05 versus Tsc1^{+/+} mice after IRI, *n* = 6. **j, k** Quantitative determination of apoptotic cells among groups. Data are presented as the number of apoptotic cells per HPF (400 \times). **P* < 0.05 versus Tsc1^{+/+} mice, *n* = 3–6; #*P* < 0.05 versus Tsc1^{+/+} mice after IRI, *n* = 6. Each dot represents the average of five HPFs from each mouse

(Supplemental Fig. 1f). Mice were operated with left renal IRI and right renal nephrectomy (Fig. 4a). Costaining results demonstrated the ablation of Rictor in fibroblasts from Gli1⁺-Rictor^{-/-} mice (Fig. 4b). At 1 day after IRI, the knockouts developed more severe kidney dysfunction and morphological damage compared to their littermate controls (Fig. 4c, d, f). Similar to those in Gli1⁺-Rheb^{-/-} mice, neutrophil and T lymphocyte infiltration, mRNA abundance for *Rantes*, *Mcp-1*, and *Tnf- α* , the number of cleaved caspase 3 and TUNEL staining positive cells were all largely

increased in Gli1⁺-Rictor^{-/-} kidneys compared to their littermate controls after IRI (Fig. 4d, e, g–k). Together, these results suggest that ablation of Rictor in fibroblasts aggravates tubular cell death and AKI in mice.

Fibroblast mTORC1 and mTORC2 activation protects against staurosporine-induced tubular cell apoptosis

The above data demonstrated that both mTORC1 and mTORC2 signaling in fibroblasts are crucial for protecting

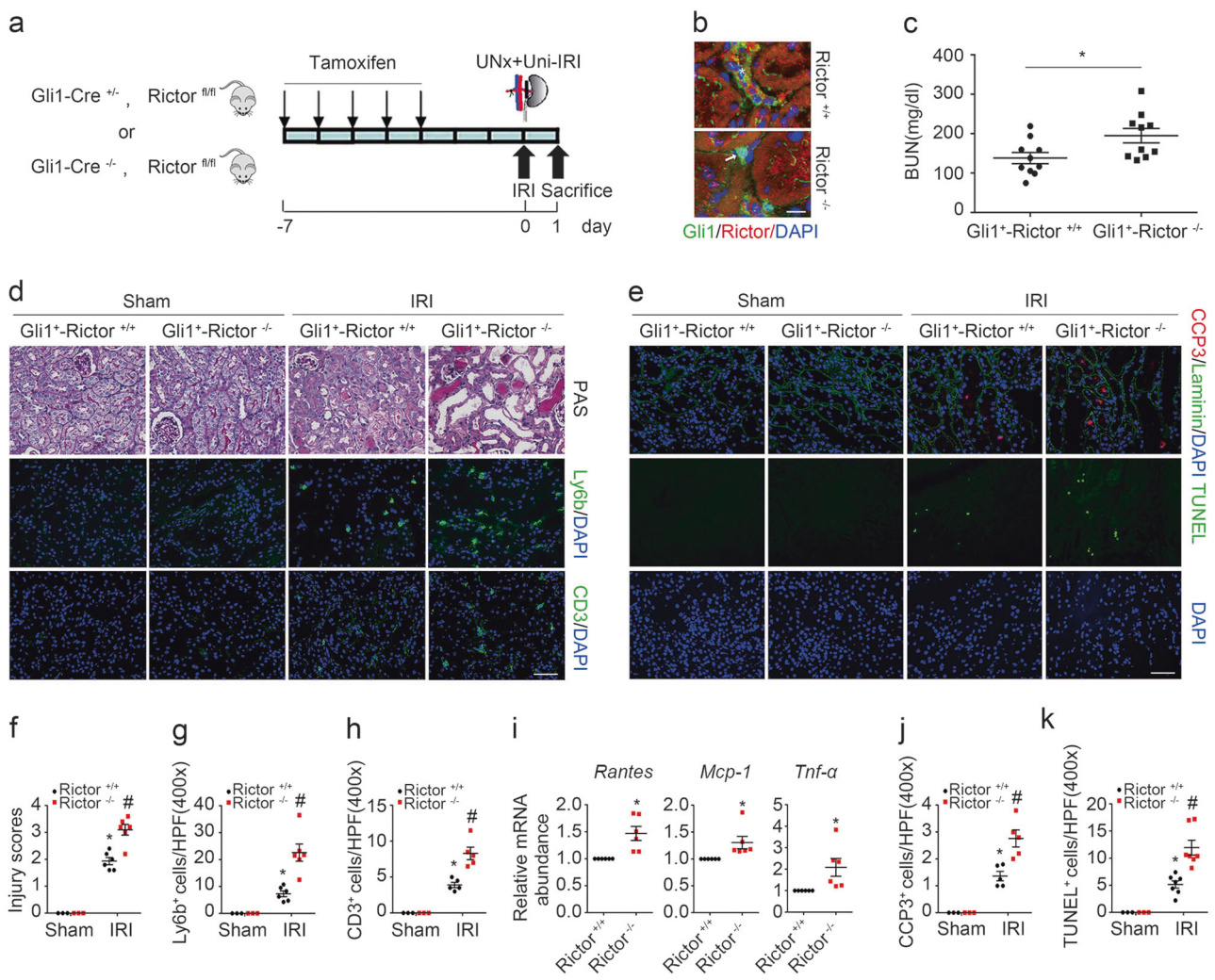


Fig. 4 Ablation of fibroblast Rictor aggravates kidney ischemia/reperfusion injury in mice. **a** The strategy for inducing fibroblast Rictor gene deletion in Gli1-Cre^{+/+}, Rictor^{fl/fl} mice and renal IRI surgery. **b** Representative micrographs showing the ablation of Rictor in Gli1⁺ cells in IRI kidneys from Gli1⁺-Rictor^{-/-} mice. The asterisk indicates both Gli1- and Rictor-positive cells in Rictor^{+/+} kidneys. The white arrow indicates Gli1-positive but Rictor-negative cells in the knockout kidneys. Scale bar = 10 μ m. **c** The graph showing blood urea nitrogen (BUN) level in Gli1⁺-Rictor^{+/+} and Gli1⁺-Rictor^{-/-} mice at 1 day after IRI. * P < 0.05, n = 10. **d** Kidney histology as shown by PAS staining. Representative immunofluorescent staining images for Ly6b and CD3 among groups as indicated. Scale bar = 50 μ m. **e** Representative immunofluorescent staining images for cleaved caspase 3 and TUNEL staining for apoptotic cells among groups as

indicated. **f** The graph showing the injury scores among groups. * P < 0.05 versus Rictor^{+/+} mice, n = 3–6; # P < 0.05 versus Rictor^{+/+} mice after IRI, n = 6. Each dot represents the average of five HPFs from each mouse. **g, h** Quantitative determination of Ly6b⁺ cells and CD3⁺ cells among groups as indicated. * P < 0.05 versus Rictor^{+/+} mice, n = 3–6; # P < 0.05 versus Rictor^{+/+} mice after IRI, n = 5–6. Each dot represents the average of four HPFs from each mouse. **i** Real-time qRT-PCR analysis showing the mRNA abundance for *Rantes*, *Mcp-1*, and *Tnf- α* in Rictor^{+/+} and the knockout kidneys at day 1 after IRI. * P < 0.05 versus Rictor^{+/+} mice after IRI, n = 6. **j, k** Quantitative determination of cleaved caspase 3⁺ cells and TUNEL⁺ cells. * P < 0.05 versus Rictor^{+/+} mice, n = 3–7; # P < 0.05 versus Rictor^{+/+} mice after IRI, n = 6–7. Each dot represents the average of five HPFs from each mouse

against tubular cell death and AKI in mice. To further investigate the role and mechanisms for fibroblast mTOR signaling in regulating tubular cell survival, we generated a coculture system of tubular cells which were incubated with CM from fibroblasts, followed by staurosporine treatment to trigger cell death (Fig. 5a). Primary cultured kidney fibroblasts from Rheb^{fl/fl}, Tsc1^{fl/fl}, and Rictor^{fl/fl} mice were infected with adenovirus carrying Cre recombinase for 48 h to induce

target gene ablation. The cells were infected with adenovirus carrying GFP and treated as control fibroblasts (Fig. 5b–d). Western blot assay showed that much more caspase 3 cleavage was detected at 1 h after staurosporine treatment in tubular cells incubated with CM from Rheb^{-/-} and Rictor^{-/-} fibroblasts compared to those incubated with CM from control fibroblasts (Fig. 5e, g). Less staurosporine-induced caspase 3 cleavage was observed in tubular cells incubated with

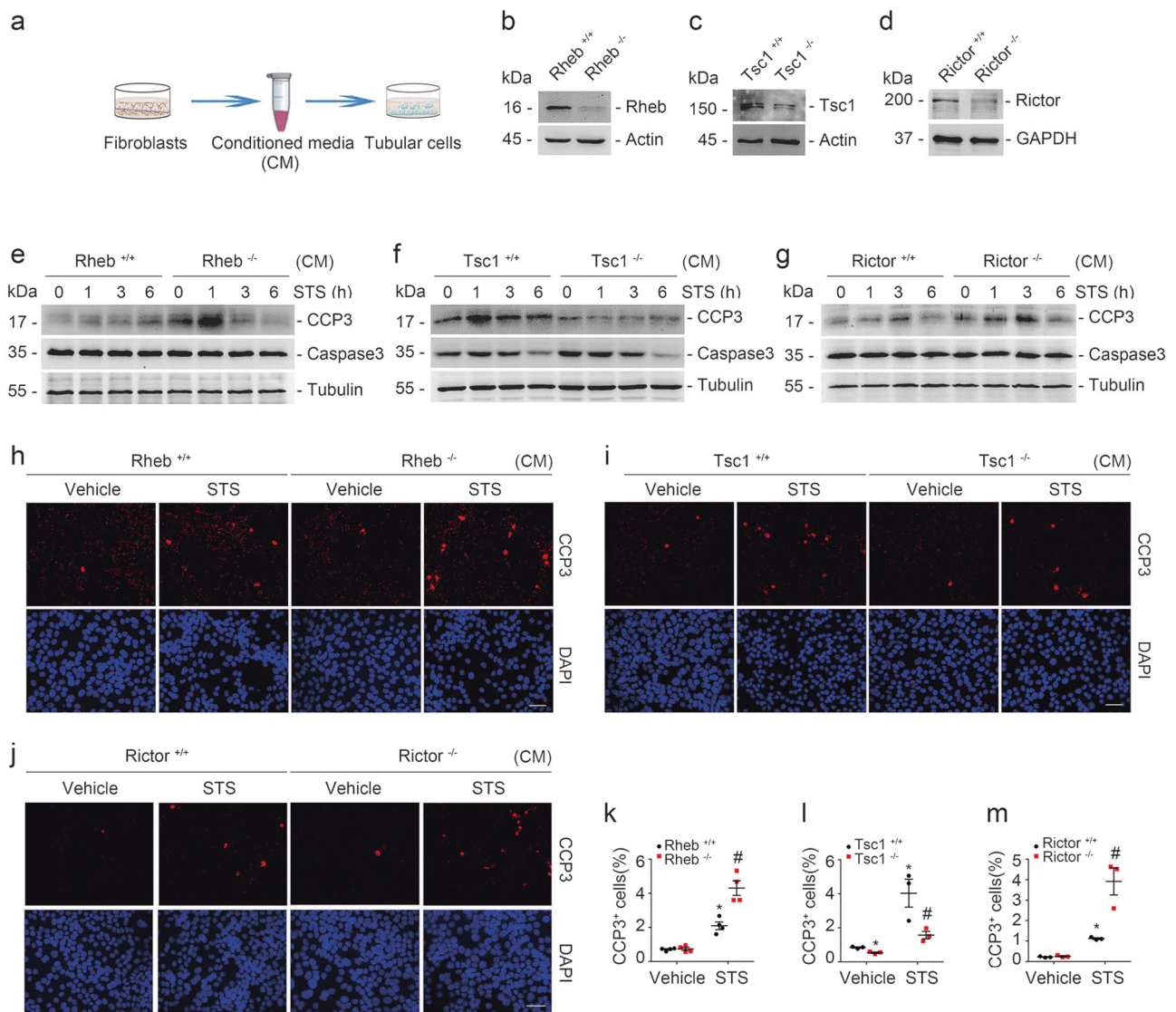


Fig. 5 Fibroblast mTORC1 and mTORC2 activation protects against staurosporine-induced tubular cell apoptosis. **a** The coculture system of tubular cells and kidney fibroblasts. **b–d** Western blot assay showing the abundance for Rheb, Tsc1, and Rictor in kidney fibroblasts. Primary cultured kidney fibroblasts generated from Rheb^{fl/fl}, Tsc1^{fl/fl}, and Rictor^{fl/fl} mice were infected with adeno-Cre for 48 h to induce Rheb, Tsc1, and Rictor gene ablation, respectively. Fibroblasts infected with adeno-GFP were used as control fibroblasts. **e–g** Western blotting analyses showing the abundance of cleaved caspase 3 in primary cultured tubular cells incubated with CM from various primary cultured kidney fibroblasts as indicated. Tubular cells were treated with staurosporine (1 μ M) for different duration. **h–j** Representative immunofluorescent staining images for cleaved caspase 3

among groups as indicated. Tubular cells were treated with staurosporine (1 μ M) for 3 h. Scale bar = 20 μ m. **k–m** Quantitative determination of cleaved caspase 3⁺ cells among groups as indicated. Data are presented as the percentage of the counted cells. * P < 0.05 versus vehicle-treated Rheb^{+/+} fibroblasts, n = 4; # P < 0.05 versus staurosporine-treated Rheb^{+/+} fibroblasts, n = 4. n = 4 refers to four independent repeats (**k**); * P < 0.05 versus vehicle-treated Tsc1^{+/+} fibroblasts, n = 3; # P < 0.05 versus staurosporine-treated Tsc1^{+/+} fibroblasts, n = 3. n = 3 refers to three independent repeats (**l**); * P < 0.05 versus vehicle-treated Rictor^{+/+} fibroblasts, n = 3; # P < 0.05 versus staurosporine-treated Rictor^{+/+} fibroblasts, n = 3. n = 3 refers to three independent repeats (**m**). CM conditioned media

CM from Tsc1^{-/-} fibroblasts compared to those incubated with CM from control fibroblasts (Fig. 5f). Immunostaining for cleaved caspase 3 further confirmed these results (Fig. 5h–m). Together, these results reveal that fibroblast mTORC1 and mTORC2 signaling activation protect against staurosporine-induced tubular cell death.

Fibroblast mTOR/PPAR γ /HGF axis promotes tubular cell survival

Previous studies demonstrated that PPAR γ functions as one of the major downstream molecules of mTOR signaling [29]. In addition, the published studies showed that PPAR γ

upregulates HGF expression, which protects against tubular cell death and AKI [30–33]. Therefore, we predicated that fibroblast mTOR signaling activation may promote tubular cell survival through PPAR γ /HGF induction. To verify this, we examined PPAR γ and HGF abundance in Rheb^{-/-}, Tsc1^{-/-}, and Rictor^{-/-} fibroblasts, respectively. Comparing to control fibroblasts, PPAR γ and *Hgf* expression were largely downregulated in Rheb^{-/-} and Rictor^{-/-} fibroblasts, and upregulated in Tsc1^{-/-} fibroblasts (Fig. 6a, b). Western blot assay showed that the abundance of p-c-met (Y1234/Y1235) and p-ERK1/2 (T202/Y204) was markedly decreased in tubular cells cultured with CM from Rheb^{-/-} or Rictor^{-/-} fibroblasts, but largely increased in those cultured with CM from Tsc1^{-/-} fibroblasts compared to control fibroblasts (Fig. 6c–e).

To evaluate the role for fibroblast PPAR γ /HGF production in regulating tubular cell survival, we treated NRK-49F cells with Pioglitazone, a PPAR γ agonist, and found that Pioglitazone could upregulate *Hgf* expression (Fig. 6f). Western blot assay showed that staurosporine-induced tubular cell apoptosis was largely attenuated in NRK-52E cells incubated with CM from Pioglitazone-treated fibroblasts (Fig. 6g). We also transfected NRK-49F cells with HGF siRNAs to downregulate *Hgf* expression (Fig. 6h). The results showed that more tubular cells incubated with CM from HGF siRNA transfected fibroblasts underwent apoptosis compared to those incubated with CM from scramble siRNA transfected fibroblasts after staurosporine treatment (Fig. 6i). To further decipher the role for HGF produced by fibroblasts in protecting against tubular cell death, we treated tubular cells with PF-04217903, an inhibitor of HGF receptor c-met, to block HGF signaling. The results showed that PF-04217903 enhanced staurosporine-induced tubular cell apoptosis (Fig. 6j). Immunostaining for cleaved caspase 3 confirmed these results (Fig. 6k–n).

In addition to ablation of mTOR signaling molecules by genetic method, we treated NRK-49F cells with PP242 to pharmacologically block mTOR signaling in the fibroblasts. PPAR γ and *Hgf* expression were markedly downregulated after PP242 treatment in NRK-49F cells (Fig. 7a, b). The abundance for p-c-met (Y1234/Y1235) and p-ERK1/2 (T202/Y204) was decreased, and more tubular cell apoptosis was detected in tubular cells cultured with CM from PP242-treated fibroblasts compared to those from vehicle-treated fibroblasts (Fig. 7c, d). Moreover, Pioglitazone could antagonize PP242-suppressed *Hgf* expression in NRK-49F cells (Fig. 7e). In NRK-52E cells, comparing to those incubated with CM from control fibroblasts, much more cell apoptosis was detected in the cells incubated with CM from PP242-treated fibroblasts, which was largely reduced in those incubated with CM from Pioglitazone-treated fibroblasts (Fig. 7f, g). Thus, it is clear that fibroblast mTOR dependent PPAR γ /HGF production facilitates

tubular cell survival through activating tubular cell c-met signaling.

MTOR upregulates PPAR γ /HGF expression in kidney fibroblasts in mice

In cultured kidney fibroblasts, blocking mTOR signaling could suppress PPAR γ /HGF production. In mouse models, PPAR γ and *Hgf* expression were largely suppressed in Gli1⁺-Rheb^{-/-} or Gli1⁺-Rictor^{-/-} kidneys compared to their littermate controls at 1 day after IRI, and markedly increased in Gli1⁺-Tsc1^{-/-} kidneys compared to their littermate controls (Fig. 8a–f).

We then stained the kidney tissues with antibody against PPAR γ and the results showed that PPAR γ was majorly expressed in kidney interstitial cells from the littermate controls, which was much less in Gli1⁺-Rheb^{-/-} and Gli1⁺-Rictor^{-/-} kidneys after IRI. Costaining results showed that PPAR γ abundance in fibroblasts from Gli1⁺-Rheb^{-/-} and Gli1⁺-Rictor^{-/-} mice was decreased compared to their littermate controls after IRI (Fig. 8g, h). In Gli1⁺-Tsc1^{-/-} kidneys, PPAR γ expression was largely upregulated in fibroblasts compared to those in their littermate control kidneys (Fig. 8i). Taken together, these results suggest that mTOR signaling activation in fibroblasts is able to upregulate PPAR γ /HGF expression in the mouse kidneys.

Interactions between Tsc1/Rheb/mTORC1 and mTORC2 signaling in kidney fibroblasts

The above data demonstrated that both mTORC1 and mTORC2 signaling in fibroblasts protect against ischemia/reperfusion-induced tubular cell death and AKI via PPAR γ /HGF induction. We then want to know whether mTORC1 and mTORC2 may interact with each other for regulating PPAR γ /HGF expression in kidney fibroblasts. In primary cultured kidney fibroblasts with Rheb or Tsc1 gene ablation, western blot assay showed that p-Akt (Ser473) abundance was not changed compared to those in control fibroblasts (Fig. 9a, b). In the kidneys from Gli1⁺-Rheb^{-/-} or Gli1⁺-Tsc1^{-/-} mice, at 1 day after IRI, no significant difference was found for p-Akt (Ser473) abundance between the knockouts and littermate controls (Fig. 9c, d).

We transfected NRK-49F cells with Raptor siRNAs to downregulate *Raptor* expression (Fig. 9e). In NRK-49F cells transfected with Raptor siRNAs, p-S6 abundance was remarkably reduced compared to those transfected with scramble siRNA (Fig. 9f). The abundance for PPAR γ and *Hgf* expression, p-c-met (Y1234/Y1235) and p-ERK1/2 (T202/Y204) was decreased and more tubular cell apoptosis was observed in tubular cells incubated with CM from Raptor siRNA transfected fibroblasts compared to those transfected with scramble siRNA (Supplemental Fig. 2).

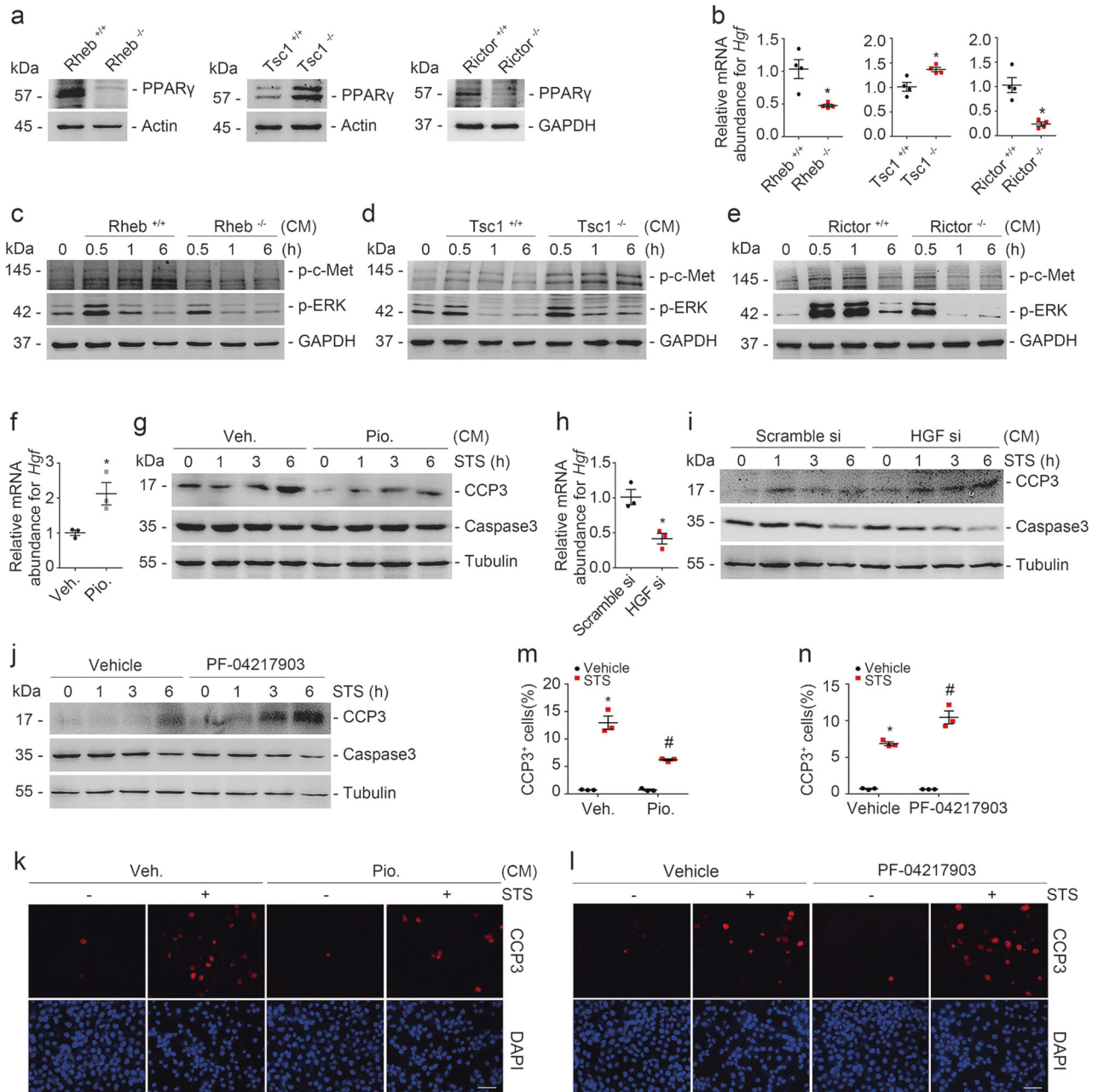


Fig. 6 Fibroblast mTOR/PPAR γ dependent HGF production promotes tubular cell survival. **a** Western blot analyses showing the abundance of PPAR γ in primary cultured Rheb $^{-/-}$, Tsc1 $^{-/-}$, and Rictor $^{-/-}$ kidney fibroblasts, respectively. **b** Real-time qRT-PCR analysis showing the mRNA abundance for *Hgf* in primary cultured kidney fibroblasts. * $P < 0.05$ versus cells infected with adenovirus carrying GFP, $n = 4$. $n = 4$ refers to four independent repeats. **c–e** Western blotting analyses showing the abundance of p-c-met (Y1234/Y1235) and p-ERK1/2 (T202/Y204) as indicated. GAPDH was probed to show the equal loading. **f** Real-time qRT-PCR analysis showing the mRNA abundance for *Hgf* in NRK-49F cells. * $P < 0.05$ versus vehicle-treated cells, $n = 3$. $n = 3$ refers to three independent repeats. NRK-49F cells were pretreated with Pioglitazone for 24 h. **g** NRK-52E cells were treated with staurosporine (1 μ M) for different duration as indicated. Western blot analyses showing the abundance of cleaved caspase 3. **h** Real-time qRT-PCR analysis showing the mRNA abundance *Hgf* in NRK-

49F cells transfected with scramble or HGF siRNA as indicated. * $P < 0.05$ versus cells transfected with scramble siRNA, $n = 3$. $n = 3$ refers to three independent repeats. **i, j** NRK-52E cells were treated with staurosporine (1 μ M) for different duration as indicated. Western blotting analysis showing that knocking down *Hgf* in NRK-49F cells (**i**) or blockade of tubular cell c-met signaling (**j**) could aggravate staurosporine-induced NRK-52E cell apoptosis. **k, l** NRK-52E cells were treated with staurosporine (1 μ M) for 3 h. Representative immunofluorescent staining images for cleaved caspase 3 among groups as indicated. Scale bar = 20 μ m. **m, n** Quantitative determination of cleaved caspase 3 $^{+}$ cells among groups as indicated. Data are presented as the percentage of the counted cells. * $P < 0.05$ versus vehicle-treated cells, $n = 3$; # $P < 0.05$ versus staurosporine-treated cells, $n = 3$. $n = 3$ refers to three independent repeats. CM conditioned media

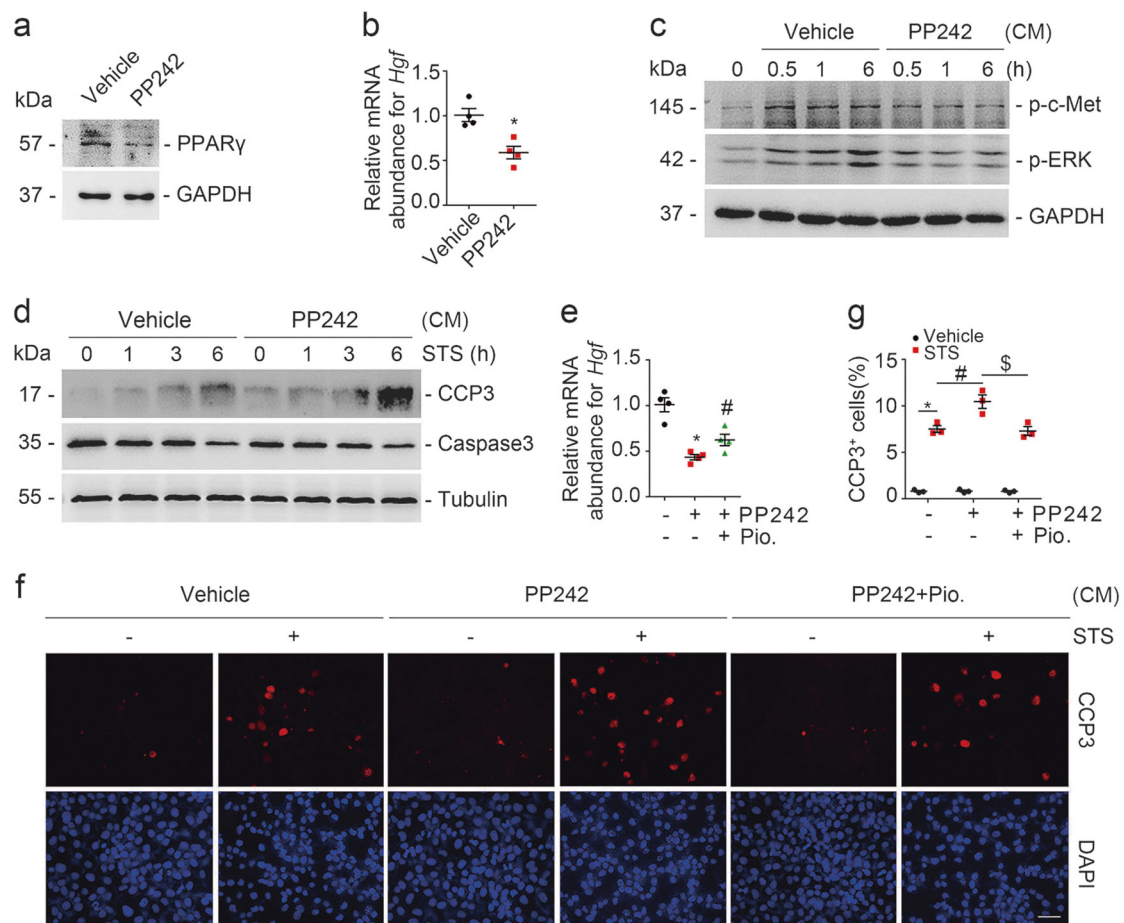


Fig. 7 Pharmacological blockade of fibroblast mTOR signaling represses HGF expression and aggravates tubular cell apoptosis. **a** Western blot analyses showing the reduction of PPAR γ in NRK-49F cells treated with PP242. **b** Real-time qRT-PCR analysis showing the mRNA abundance for *Hgf* in NRK-49F cells. * $P < 0.05$ versus vehicle-treated cells, $n = 4$. $n = 4$ refers to four independent repeats. **c** Western blot analyses showing the abundance of p-c-met (Y1234/Y1235) and p-ERK1/2 (T202/Y204) as indicated. GAPDH was probed to show the equal loading. **d** NRK-52E cells were treated with staurosporine (1 μ M) for different duration as indicated. Western blot analyses showing the abundance of cleaved caspase 3 in NRK-52E cells incubated with CM from PP242-treated NRK-49F cells. **e** Real-time qRT-PCR analysis showing that Pioglitazone could restore the

mRNA abundance of *Hgf* suppressed by PP242 administration. * $P < 0.05$ versus vehicle-treated cells, $n = 4$; # $P < 0.05$ versus PP242-treated cells, $n = 4$. $n = 4$ refers to four independent repeats. **f** NRK-52E cells were treated with staurosporine (1 μ M) for 3 h. Representative immunofluorescent staining images for cleaved caspase 3 among groups as indicated. Scale bar = 20 μ m. **g** Quantitative determination of cleaved caspase 3⁺ cells among groups as indicated. Data are presented as the percentage of the counted cells. * $P < 0.05$ versus vehicle-treated cells, $n = 3$; # $P < 0.05$ versus staurosporine-treated cells that were incubated with CM from vehicle-treated fibroblasts, $n = 3$; \$ $P < 0.05$ versus staurosporine-treated cells that were incubated with CM from PP242-treated fibroblasts, $n = 3$. $n = 3$ refers to three independent repeats. CM conditioned media

We treated NRK-49F cells with rapamycin to pharmacologically block mTORC1 signaling. The results showed that rapamycin could largely reduce S6 phosphorylation, whereas the abundance for p-Akt (Ser473) remained unchanged (Fig. 9g). Rapamycin could markedly decrease PPAR γ and *Hgf* expression in NRK-49F cells (Supplemental Fig. 3a, b). The abundance for p-c-met (Y1234/Y1235) and p-ERK1/2 (T202/Y204) was decreased and cell apoptosis was enhanced in tubular cells incubated with CM from rapamycin-treated fibroblasts compared to vehicle-treated fibroblasts (Supplemental Fig. 3c–f). Put all

together, it is concluded that Tsc1/Rheb/mTORC1 does not affect mTORC2 signaling activation in kidney fibroblasts.

In the primary cultured kidney fibroblasts with Rictor gene ablation, western blot assay showed that ablation of Rictor could largely reduce p-S6 abundance (Fig. 10a). In Gli1⁺-Rictor^{-/-} mouse kidneys, at 1 day after IRI, p-S6 abundance was markedly decreased compared to their littermate controls (Fig. 10b). We costained the kidney tissues with antibodies against PDGFR β and p-S6. The p-S6 abundance was decreased in the fibroblasts from the knockout kidneys after IRI (Fig. 10c). These results suggest

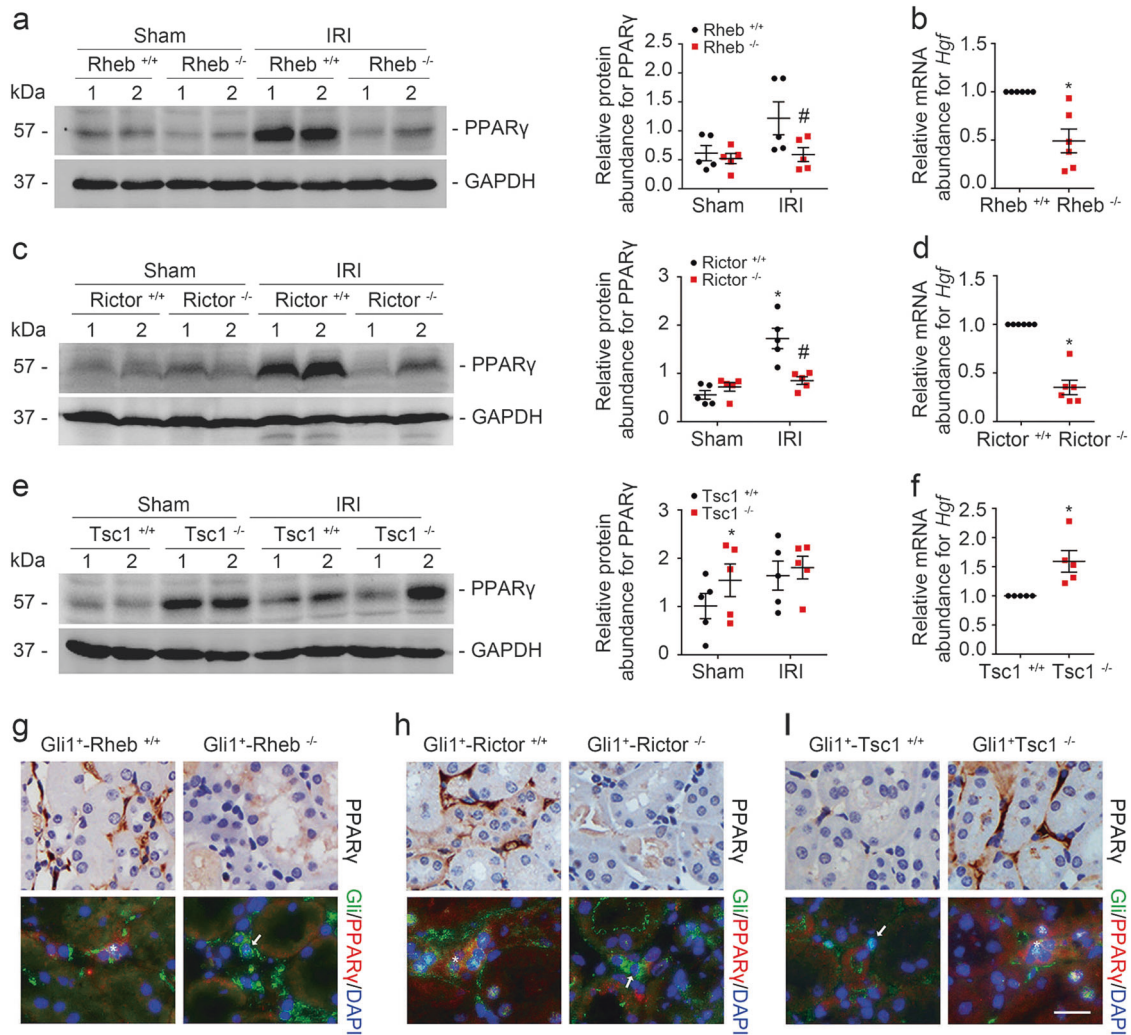


Fig. 8 MTOR regulates PPAR γ /HGF expression in kidney fibroblasts in mice. **a, c, e** Western blot analyses showing the PPAR γ abundance in the sham and IRI kidneys from the knockouts and littermate controls. Numbers indicate each individual animal within each group (left). The graphs showing the quantification of the PPAR γ in the IRI and sham kidneys. **P* < 0.05 versus littermate controls, #*P* < 0.05 versus littermate controls after IRI, *n* = 5. **b, d, f** Real-time qRT-PCR

analysis showing the mRNA abundance for *Hgf* in the knockout and littermate control kidneys. **P* < 0.05 versus WT mice, *n* = 5–6. **g–i** Immunostaining showing PPAR γ in the interstitial cells among groups as indicated. The asterisk indicates both Gli1- and PPAR γ -positive cells in the Rheb^{+/+}, Rictor^{+/+}, and Tsc1^{-/-} kidneys. The arrow indicates Gli1-positive but PPAR γ -negative cells in the Rheb^{-/-}, Rictor^{-/-}, and Tsc1^{+/+} kidneys. Scale bar = 20 μ m

that mTORC2 signaling is indispensable for mTORC1 signaling activation in the kidney fibroblasts.

Discussion

We report here that fibroblast mTORC1 and mTORC2 signaling are crucial for protecting against tubular cell death and AKI, which is through upregulating PPAR γ and HGF expression. To our knowledge, this study decipheres a unique role and mechanism for fibroblast mTOR signaling in regulating tubular cell survival and AKI.

Although several molecules such as Gli1, Fsp1, and PDGFR β have been reported to be expressed in

fibroblasts/pericytes, there is no specific biomarker that can distinguish interstitial fibroblasts from capillary pericytes. Therefore, “fibroblasts,” a broad term including both interstitial fibroblast and pericyte was used in this study. In IRI-induced AKI model, Gli1⁺ fibroblast loss induces capillary rarefaction and proximal tubular injury, suggesting a crucial role for Gli1⁺ fibroblasts in the pathogenesis of AKI [11]. We demonstrated here that Gli1⁺ fibroblast mTOR signaling is vital for promoting tubular cell survival in IRI-induced AKI based on several lines of evidence. First, both mTORC1 and mTORC2 were activated in kidney fibroblasts after IRI. Second, ablation of fibroblast Rheb or Rictor aggravated tubular cell death and IRI. While ablation of fibroblast Tsc1

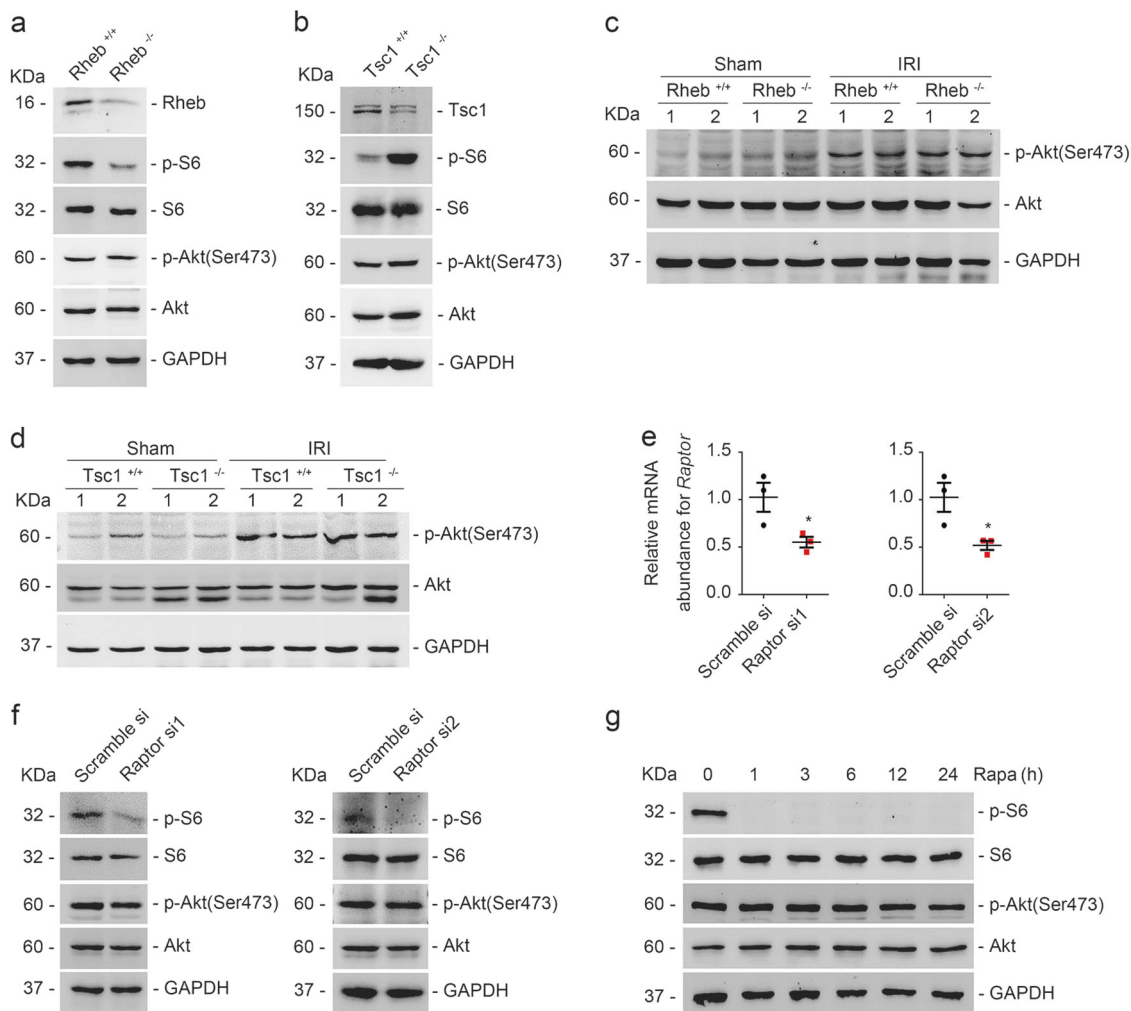


Fig. 9 Tsc1/Rheb/mTORC1 does not affect mTORC2 signaling activation in kidney fibroblasts. **a, b** The primary cultured kidney fibroblasts generated from Rheb^{fl/fl}, or Tsc1^{fl/fl} mice were infected with adeno-Cre virus to induce Rheb, or Tsc1 gene deletion. Western blotting assay showing that ablation of Rheb or Tsc1 could not affect the p-Akt (Ser473) abundance. **c, d** Western blot analyses showing p-Akt (Ser473) abundance in the Sham and IRI kidneys. Numbers indicate each individual animal within each group. **e** Real-time qRT-

PCR analysis showing *Raptor* mRNA abundance in NRK-49F cells transfected with scramble or Raptor siRNA as indicated. **P* < 0.05 versus cells transfected with scramble siRNA, *n* = 3. *n* = 3 refers to three independent repeats. **f** Western blotting analyses showing that knocking down *Raptor* expression inhibited S6 phosphorylation but not Akt phosphorylation at Ser473. **g** Western blot analyses showing the abundance of p-S6 and p-Akt (Ser473) in NRK-49F cells after rapamycin treatment

protected against tubular cell death and IRI. Third, CM from Rheb^{-/-} or Rictor^{-/-} kidney fibroblasts aggravated staurosporine-induced tubular cell apoptosis, and CM from Tsc1^{-/-} kidney fibroblasts promoted tubular cell survival. It should be pointed out that the protective effect of fibroblast mTOR signaling on tubular survival may be underestimated because only 43% of the kidney interstitial cells are Gli1-positive after IRI [11, 13].

Upon kidney injury, fibroblasts undergo proliferation, activation, and migration toward the injury area, where they may support tubular cell dedifferentiation, proliferation, and regeneration [12, 34, 35]. After injury, activated fibroblasts may be eliminated through death, senescence and

dedifferentiation. However, sustained activation of fibroblasts in the kidney tissue may lead to interstitial extracellular matrix deposition and kidney fibrosis [36, 37]. The mTOR kinase is an evolutionarily conserved member of the phosphatidylinositol-3-OH (PI-3)-kinase-related kinase (PI3KK) family, which plays an essential role in various biological processes, including cell survival, proliferation and metabolism [38]. In this study, we found that fibroblast mTOR signaling activation protected against IRI-induced tubular cell death and AKI. Previous studies demonstrated that continuous mTOR signaling activation in fibroblasts may lead to fibroblast differentiation and kidney fibrosis [24, 25]. Therefore, it may be concluded that fibroblast

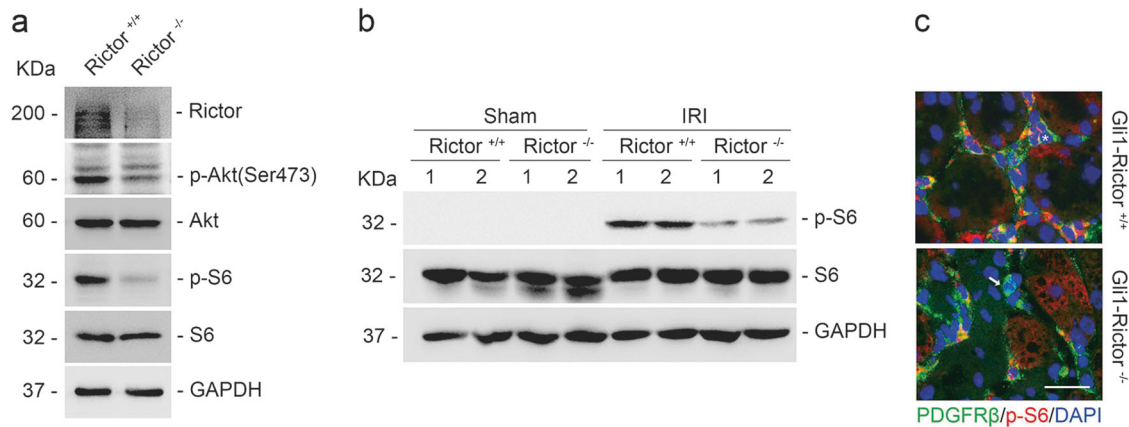


Fig. 10 mTORC2 is indispensable for mTORC1 signaling activation in kidney fibroblasts. **a** Western blot assay showing that ablation of Rictor reduced p-S6 abundance in kidney fibroblasts. The primary cultured fibroblasts generated from the kidneys of Rictor^{fl/fl} mice were infected with adeno-Cre virus to induce Rictor gene deletion. **b** Western blot analyses showing p-S6 abundance in the Sham and IRI

kidneys. Numbers indicate each individual animal within each group. **c** Representative images showing the less induction of p-S6 in the kidney fibroblasts from Gli1⁺-Rictor^{-/-} mice at day 1 after IRI. The asterisk indicates both PDGFR β - and p-S6-positive cells in littermate control kidneys. The arrow indicates PDGFR β -positive but p-S6-negative cells in the knockout kidneys. Scale bar = 20 μ m

mTOR signaling plays a dual role during kidney injury. At the early stage of the AKI, fibroblast mTOR signaling activation is beneficial, while continuing activation of mTOR signaling in fibroblasts may lead to extracellular matrix deposition and kidney fibrosis. The mechanisms for regulating fibroblast mTOR signaling activation during AKI to CKD transition remain to be elucidated.

In renal interstitium, multiple soluble factors mediate the communication between fibroblasts and tubular cells [39, 40]. Among of them, HGF produced by mesenchymal cells protects against tubular cell death through binding and triggering the HGF receptor c-met activation [41–45]. It has been reported that mTORC1 signaling activation may upregulate PPAR γ expression in various cell types [22, 29, 46–48]. And HGF is transcriptionally upregulated by PPAR γ in mesenchymal cells [32]. In this study, we found that both mTORC1 and mTORC2 could stimulate PPAR γ and HGF expression in kidney fibroblasts. In both animal models and cultured cells, we found that HGF mediated the protective effect of fibroblast mTOR signaling on tubular cell death. In mouse models, ablation of Rheb or Rictor in fibroblasts reduced while ablation of Tsc1 in fibroblasts increased PPAR γ and *Hgf* abundance. In cultured kidney fibroblasts, similar results were observed. Pioglitazone could markedly upregulate *Hgf* expression in fibroblasts and the CM from Pioglitazone-treated fibroblasts diminished staurosporine-induced tubular cell death. Furthermore, downregulating fibroblast HGF expression or blockade of tubular cell c-met signaling promoted staurosporine-induced tubular cell apoptosis. Thus, this study demonstrated that fibroblast mTOR/PPAR γ dependent HGF production is essential for promoting tubular cell survival after IRI.

In HeLa cells, Liu et al. reported that mTORC1 inhibits mTORC2 signaling through phosphorylating Sin1 [49]. In NK cells, Wang et al. demonstrated that mTORC1 sustains mTORC2 activity, while mTORC2 negatively regulates mTORC1 signaling activation. These observations suggest that the interaction between mTORC1 and mTORC2 exhibits a context-dependent manner [50]. In primary cultured kidney fibroblasts, we found that ablation of Rheb or Tsc1 could not alter the p-Akt (Ser473) abundance. Consistently, in mouse models, ablation of fibroblast Rheb or Tsc1 could not affect the abundance of p-Akt (Ser473). Therefore, it may be concluded that Rheb or Tsc1 does not affect mTORC2 signaling in kidney fibroblasts. In addition, in NRK-49F cells, downregulating Raptor expression or blocking mTORC1 signaling with rapamycin could not affect Akt phosphorylation at Ser473. While ablation of Rictor in primary cultured kidney fibroblasts largely decreased the p-S6 abundance. In kidney fibroblasts, mTORC2 positively regulates mTORC1 signaling, but not vice versa.

In summary, we report here that fibroblast mTOR signaling activation protects against IRI-induced AKI via PPAR γ and HGF induction. Targeting fibroblast mTOR signaling may offer a new strategy for protecting against tubular cell death and AKI.

Acknowledgements This work was supported by National Science Foundation of China Grants 81570611/H0503, 81770675/H0503 and Science Foundation of Jiangsu Province Grants BK20140048 to CD.

Author contributions YG, QL, MG, MW, YL, XZ, XX and XS performed the experiments. YG wrote the manuscript. JY and WH analyzed the data. AZ and BX provided the reagents and analyzed the data. CD designed, supervised, and revised the manuscript.

Compliance with ethical standards

Conflict of interest The authors declare that they have no conflict of interest.

Publisher's note: Springer Nature remains neutral with regard to jurisdictional claims in published maps and institutional affiliations.

References

- Mehta R, Cerdá J, Burdman E, Tonelli M, García-García G, Jha V, et al. International Society of Nephrology's Oby25 initiative for acute kidney injury (zero preventable deaths by 2025): a human rights case for nephrology. *Lancet*. 2015;385:2616–43.
- Devarajan P. Update on mechanisms of ischemic acute kidney injury. *J Am Soc Nephrol*. 2006;17:1503–20.
- Bonventre JV, Yang L. Cellular pathophysiology of ischemic acute kidney injury. *J Clin Investig*. 2011;121:4210–21.
- Sharfuddin AA, Molitoris BA. Pathophysiology of ischemic acute kidney injury. *Nat Rev Nephrol*. 2011;7:189–200.
- Bonventre J. Dedifferentiation and proliferation of surviving epithelial cells in acute renal failure. *J Am Soc Nephrol*. 2003;14 (Suppl 1):S55–61.
- Humphreys B, Czerniak S, DiRocco D, Hasnain W, Cheema R, Bonventre J. Repair of injured proximal tubule does not involve specialized progenitors. *Proc Natl Acad Sci USA*. 2011;108:9226–31.
- Humphreys B, Valerius M, Kobayashi A, Mugford J, Soeung S, Duffield J, et al. Intrinsic epithelial cells repair the kidney after injury. *Cell Stem Cell*. 2008;2:284–91.
- Lieberthal W, Levine JS. Mechanisms of apoptosis and its potential role in renal tubular epithelial cell injury. *Am J Physiol*. 1996;271:F477–88.
- Kaissling B, Le Hir M. The renal cortical interstitium: morphological and functional aspects. *Histochem Cell Biol*. 2008;130:247–62.
- Takahashi-Iwanaga H. The three-dimensional cytoarchitecture of the interstitial tissue in the rat kidney. *Cell Tissue Res*. 1991;264:269–81.
- Kramann R, Wongboonsin J, Chang-Panesso M, Machado FG, Humphreys BD. Gli1(+) pericyte loss induces capillary rarefaction and proximal tubular injury. *J Am Soc Nephrol*. 2017;28:776–84.
- Schiessl IM, Grill A, Fremter K, Steppan D, Hellmuth MK, Castrop H. Renal interstitial platelet-derived growth factor receptor-beta cells support proximal tubular regeneration. *J Am Soc Nephrol*. 2018;29:1383–96.
- Zhou D, Fu H, Xiao L, Mo H, Zhuo H, Tian X, et al. Fibroblast-specific beta-catenin signaling dictates the outcome of AKI. *J Am Soc Nephrol*. 2018;29:1257–71.
- Johnson SC, Rabinovitch PS, Kaerberlein M. mTOR is a key modulator of ageing and age-related disease. *Nature*. 2013;493:338–45.
- Stanfel MN, Shamieh LS, Kaerberlein M, Kennedy BK. The TOR pathway comes of age. *Biochim Biophys Acta*. 2009;1790:1067–74.
- Peterson TR, Laplante M, Thoreen CC, Sancak Y, Kang SA, Kuehl WM, et al. DEPTOR is an mTOR inhibitor frequently overexpressed in multiple myeloma cells and required for their survival. *Cell*. 2009;137:873–86.
- Saucedo LJ, Gao X, Chiarelli DA, Li L, Pan D, Edgar BA. Rheb promotes cell growth as a component of the insulin/TOR signaling network. *Nat Cell Biol*. 2003;5:566–71.
- Yamagata K, Sanders LK, Kaufmann WE, Yee W, Barnes CA, Nathans D, et al. rheb, a growth factor- and synaptic activity-regulated gene, encodes a novel Ras-related protein. *J Biol Chem*. 1994;269:16333–9.
- Tee AR, Manning BD, Roux PP, Cantley LC, Blenis J. Tuberous sclerosis complex gene products, Tuberin and Hamartin, control mTOR signaling by acting as a GTPase-activating protein complex toward Rheb. *Curr Biol*. 2003;13:1259–68.
- Inoki K, Li Y, Zhu T, Wu J, Guan KL. TSC2 is phosphorylated and inhibited by Akt and suppresses mTOR signalling. *Nat Cell Biol*. 2002;4:648–57.
- Sarbasov DD, Ali SM, Kim DH, Guertin DA, Latek RR, Erdjument-Bromage H, et al. Rictor, a novel binding partner of mTOR, defines a rapamycin-insensitive and raptor-independent pathway that regulates the cytoskeleton. *Curr Biol*. 2004;14:1296–302.
- Grahammer F, Haenisch N, Steinhart F, Sander L, Roerden M, Arnold F, et al. mTORC1 maintains renal tubular homeostasis and is essential in response to ischemic stress. *Proc Natl Acad Sci USA*. 2014;111:2817–26.
- Li J, Xu Z, Jiang L, Mao J, Zeng Z, Fang L, et al. Rictor/mTORC2 protects against cisplatin-induced tubular cell death and acute kidney injury. *Kidney Int*. 2014;86:86–102.
- Jiang L, Xu L, Mao J, Li J, Fang L, Zhou Y, et al. Rheb/mTORC1 signaling promotes kidney fibroblast activation and fibrosis. *J Am Soc Nephrol*. 2013;24:1114–26.
- Li J, Ren J, Liu X, Jiang L, He W, Yuan W, et al. Rictor/mTORC2 signaling mediates TGFβ1-induced fibroblast activation and kidney fibrosis. *Kidney Int*. 2015;88:515–27.
- Zou J, Zhou L, Du XX, Ji Y, Xu J, Tian J, et al. Rheb1 is required for mTORC1 and myelination in postnatal brain development. *Dev Cell*. 2011;20:97–108.
- Ahn S, Joyner AL. Dynamic changes in the response of cells to positive hedgehog signaling during mouse limb patterning. *Cell*. 2004;118:505–16.
- Zhou D, Li Y, Lin L, Zhou L, Igarashi P, Liu Y. Tubule-specific ablation of endogenous beta-catenin aggravates acute kidney injury in mice. *Kidney Int*. 2012;82:537–47.
- Li Z, Xu G, Qin Y, Zhang C, Tang H, Yin Y, et al. Ghrelin promotes hepatic lipogenesis by activation of mTOR-PPARγ signaling pathway. *Proc Natl Acad Sci USA*. 2014;111:13163–8.
- Herrero-Fresneda I, Torras J, Franquesa M, Vidal A, Cruzado JM, Lloberas N, et al. HGF gene therapy attenuates renal allograft scarring by preventing the profibrotic inflammatory-induced mechanisms. *Kidney Int*. 2006;70:265–74.
- Zhang J, Yang J, Liu Y. Role of Bcl-xL induction in HGF-mediated renal epithelial cell survival after oxidant stress. *Int J Clin Exp Pathol*. 2008;1:242–53.
- Li Y, Wen X, Spataro BC, Hu K, Dai C, Liu Y. Hepatocyte growth factor is a downstream effector that mediates the antifibrotic action of peroxisome proliferator-activated receptor-γ agonists. *J Am Soc Nephrol*. 2006;17:54–65.
- Dai C, Yang J, Liu Y. Single injection of naked plasmid encoding hepatocyte growth factor prevents cell death and ameliorates acute renal failure in mice. *J Am Soc Nephrol*. 2002;13:411–22.
- Sun DF, Fujigaki Y, Fujimoto T, Yonemura K, Hishida A. Possible involvement of myofibroblasts in cellular recovery of uranyl acetate-induced acute renal failure in rats. *Am J Pathol*. 2000;157:1321–35.
- Fujigaki Y, Muranaka Y, Sun D, Goto T, Zhou H, Sakakima M, et al. Transient myofibroblast differentiation of interstitial fibroblastic cells relevant to tubular dilatation in uranyl acetate-induced acute renal failure in rats. *Virchows Arch*. 2005;446:164–76.
- Yang L, Humphreys BD, Bonventre JV. Pathophysiology of acute kidney injury to chronic kidney disease: maladaptive repair. *Contrib Nephrol*. 2011;174:149–55.

37. Jun JJ, Lau LF. Resolution of organ fibrosis. *J Clin Investig.* 2018;128:97–107.
38. Beauchamp EM, Plataniotis LC. The evolution of the TOR pathway and its role in cancer. *Oncogene.* 2013;32:3923–32.
39. Imberti B, Morigi M, Tomasoni S, Rota C, Corna D, Longaretti L, et al. Insulin-like growth factor-1 sustains stem cell mediated renal repair. *J Am Soc Nephrol.* 2007;18:2921–8.
40. Tögel F, Cohen A, Zhang P, Yang Y, Hu Z, Westenfelder C. Autologous and allogeneic marrow stromal cells are safe and effective for the treatment of acute kidney injury. *Stem Cells Dev.* 2009;18:475–85.
41. Liu Y. Hepatocyte growth factor and the kidney. *Curr Opin Nephrol Hypertens.* 2002;11:23–30.
42. Matsumoto K, Nakamura T. Hepatocyte growth factor: renotropic role and potential therapeutics for renal diseases. *Kidney Int.* 2001;59:2023–38.
43. Vargas GA, Hoefflich A, Jehle PM. Hepatocyte growth factor in renal failure: promise and reality. *Kidney Int.* 2000;57:1426–36.
44. Liu Y. Hepatocyte growth factor in kidney fibrosis: therapeutic potential and mechanisms of action. *Am J Physiol Ren Physiol.* 2004;287:F7–16.
45. Zhou D, Tan RJ, Lin L, Zhou L, Liu Y. Activation of hepatocyte growth factor receptor, c-met, in renal tubules is required for renoprotection after acute kidney injury. *Kidney Int.* 2013;84:509–20.
46. Lamming DW, Demirkan G, Boylan JM, Mihaylova MM, Peng T, Ferreira J, et al. Hepatic signaling by the mechanistic target of rapamycin complex 2 (mTORC2). *FASEB J.* 2014;28:300–15.
47. Kim JE, Chen J. regulation of peroxisome proliferator-activated receptor-gamma activity by mammalian target of rapamycin and amino acids in adipogenesis. *Diabetes.* 2004;53:2748–56.
48. Angela M, Endo Y, Asou HK, Yamamoto T, Tumes DJ, Tokuyama H, et al. Fatty acid metabolic reprogramming via mTOR-mediated inductions of PPAR γ directs early activation of T cells. *Nat Commun.* 2016;7:13683.
49. Liu P, Gan W, Inuzuka H, Lazorchak AS, Gao D, Arojo O, et al. Sin1 phosphorylation impairs mTORC2 complex integrity and inhibits downstream Akt signalling to suppress tumorigenesis. *Nat Cell Biol.* 2013;15:1340–50.
50. Wang F, Meng M, Mo B, Yang Y, Ji Y, Huang P, et al. Crosstalks between mTORC1 and mTORC2 variagate cytokine signaling to control NK maturation and effector function. *Nat Commun.* 2018;9:4874.